Conformal Transformation Technique for Prediction of the Magnetic Field Distribution in an IPM Motor

Liang Fang, Soon-O Kwon, Jung-Pyo Hong
Dept. of Electrical Engineering, Changwon National University
Sarimdong 9# Changwon, Gyeongnam, 641-773, Korea

Abstract— **An analytical method used to predict the magnetic field in an interior permanent magnet (IPM) motor, is developed and validated in this paper. By using space harmonic analysis and conformal transformation (or conformal mapping (CM)) techniques, the air-gap magnetic field distribution, with considering of stator slots effect and rotor saliency effect, is precisely calculated. The accuracy of this analytical method is confirmed by the 2-dimensional finite element analysis (FEA). The analytical method can produces results much faster than FEA alone.**

I. INTRODUCTION

Interior permanent magnet (IPM) machines are well known and have been used in a variety of important applications, especially in variable-speed control system. IPM machines have some superior advantages due to their unique rotor structures, such as high torque and power density, adapting to flux-weakening operation in high speed, reduced permanent magnet (PM) requirements [1], [2].

The IPM motor is generally divided into stator part and rotor part. The stator is the same with the conventional surface PM motor, and the rotor part is composed of inserted permanent magnets and buried air-gaps, called flux barrier areas [2]. Because of the unique interior structure of the rotor, the separation of PM caused by the centrifugal force at high speed can be avoided because the PM is inserted into the rotor core, and on the other hand, IPM motor exhibits two torque components: PM torque produced by inserted PM, and reluctance torque dues to the rotor magnetic saliency, thus it exhibits a high torque-to-volume ratio [1]- [3].

The field characteristics of IPM motors are quite sensitive to the geometry of stator and rotor due to the small air-gap [1]. For this reason, in this developed analytical method, for precisely predicting the magnetic field distribution, the rotor saliency effect on the effective air-gap distribution and stator slot openings effect on the flux density distribution are taken into account, which are respectively considered by introducing the concept of "relative permeance". And both of them are dealt with conformal mapping (CM) method, which is a kind of transformation technique in essence. In this paper, the advantage of adopting CM techniques is observed from results comparison with the "assumed field pattern" used for approximate calculation mentioned in [1], [3]-[5].

The results yielded by the developed analytical method are verified by comparison with those obtained from 2-demensional (2-D) finite element analysis (FEA).

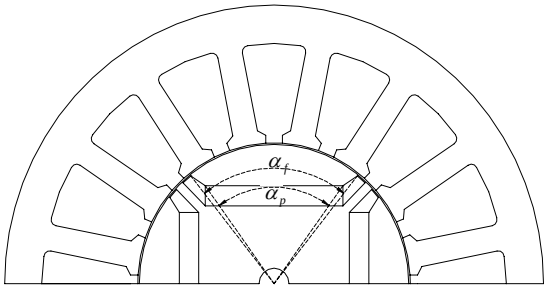

Fig.1. IPM model configuration

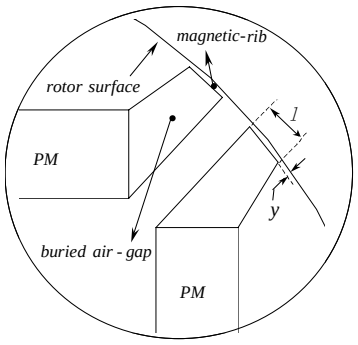

Fig.2. Flux barrier area in IPM rotor interior

II. MAGNETIC FIELD ANALYSIS

A. Descriptions of Model and Assumptions

Fig. 1 shows the topology of an IPM model. It has 4-poles and 16-slots, with parallel magnetization PMs. In order to simplify the magnetic field calculation, the following assumptions are made first [2], [4]-[5]:

a) Saturation effect is not considered (with exception for the magnetic ribs areas).
b) The slot openings are simplified to a rectangular shape.
c) The magnetic field distribution in the air-gap is determined from the product of the magnetic field produced by magnets and relative permeance.
d) The magnetic field developed by the magnets is obtained from 2-D solution of Poisson's equations by assuming a smooth stator surface, i.e. slotting is neglected.

B. Magnetic Fields in IPM

In the IPM model, flux dispersion is developing in the air-gap because the magnet flux passes through rotor core, that makes sure flux radially enters into the air-gap field,

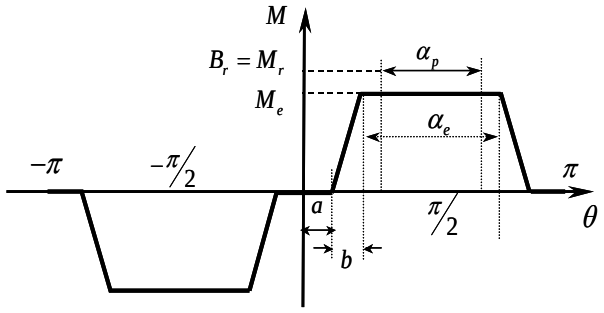

Fig.3. Magnetization distribution of inserted PM

and leakage flux exists in the flux barrier regions and magnetic ribs areas, where the iron saturation effect is included in the equivalent magnetization expression. [1].

The magnetization $\overrightarrow{M}$ with considering fringing and leakage effect, as shown in Fig. 3, represented by a Fourier series expansion is given as follow [1], [4]:

$$\overrightarrow{M} = M_r \vec{r} = \sum_{n=1,3,5...}^{\infty} M_n \sin(np\theta)\cdot\vec{r} \tag{1}$$

$$M_n = \frac{-2M_e}{bn^2\pi}[\sin(an)\{1-(-1)^n\}+\sin(n[a+b])\{-1+(-1)^n\}] \tag{2}$$

$$\overrightarrow{M}(\theta) = \sum_{n=1,3,5...}^{\infty} \frac{-4M_e}{bn^2\pi}[\sin(an)-\sin(n[a+b])]\cdot\sin(np\theta) \tag{3}$$

The flux flowing through the magnetic ribs areas is a leakage flux, where it is assumed to saturate at a constant flux density B_s. In this paper, B_s is set to about 2.0 (T). It is obtain from the *B-H* characteristics of rotor core.

Then the coefficients used for expressing the equivalent magnetization are calculated as following [1]:

$$k_1 = \frac{\alpha_f}{\alpha_p} \tag{4}$$

$$k_2 = \frac{1}{k_1}\left(1-\frac{\psi_l}{\psi_r}\right) \tag{5}$$

$$b = \alpha_p \cdot \frac{\psi_l}{\psi_r} \tag{6}$$

where $\psi_r = B_r \cdot S$, $\psi_l = B_s \cdot L \cdot y$: ψ_r is magnet flux, ψ_l is leakage flux in magnetic ribs areas, and S is magnet area, as Fig. 2 shows.

The magnetic field is obtained from equivalent magnetization, and radial component of flux density in air-gap is obtained from Poisson's equation [4], [5]. The air-gap flux density distribution according to assumption (d) is given by:

$$\frac{\partial^2\varphi}{\partial r^2}+\frac{1}{r}\frac{\partial\varphi}{\partial r}+\frac{1}{r^2}\frac{\partial^2\varphi}{\partial\theta^2}=0 \qquad \text{(in the air-gap region)} \tag{7}$$

$$\frac{\partial^2\varphi}{\partial r^2}+\frac{1}{r}\frac{\partial\varphi}{\partial r}+\frac{1}{r^2}\frac{\partial^2\varphi}{\partial\theta^2}=\frac{1}{r}\frac{M_r}{\mu_r} \quad \text{(in the magnet region)} \tag{8}$$

$$B_{gr}(r,\theta) = \sum_{n=1,3,5...}^{\infty} \frac{\mu_0 M_n}{\mu_r}\frac{np}{(np)^2-1}R_r^{-(np-1)}\cdot A \cdot[r^{(np-1)}+R_s^{2np}r^{-(np+1)}]\sin(np\theta) \tag{9}$$

$$B_{g\theta}(r,\theta) = \sum_{n=1,3,5...}^{\infty} (-1)\cdot\frac{\mu_0 M_n}{\mu_r}\frac{np}{(np)^2-1}R_r^{-(np-1)}\cdot A \cdot[r^{(np-1)}-R_s^{2np}r^{-(np-1)}]\cos(np\theta) \tag{10}$$

$$R_m = R_r - h_m \tag{11}$$

$$A = \frac{\left[(np-1)R_r^{2np}+2R_m^{np+1}R_r^{np-1}-(np+1)R_m^{2np}\right]}{\left[\frac{\mu_r+1}{\mu_r}[R_s^{2np}-R_m^{2np}]-\frac{\mu_r-1}{\mu_r}[R_r^{2np}-R_s^{2np}(R_m/R_r)^{2np}]\right]} \tag{12}$$

where B_{gr} is the radial component of flux density and $B_{g\theta}$ is the tangential component.

C. Relative Permeance Distribution

According to assumption (c), the flux density distribution in the air-gap is expressed as the product of magnet flux density and corresponding relative permeance. The relative permeance function of this presented analytical method is defined as follows [3], [6]:

$$\lambda_{total} = \lambda_{rotor-saliency} \times \lambda_{stator-slots} \tag{13}$$

The influence of stator slots in the magnetic field distribution and rotor saliency in air-gap is considered by $\lambda_{rotor-saliency}$ and $\lambda_{stator-slots}$ respectively. In this paper, CM method is applied to estimate these two considerations.

CM technique is a powerful analytical tool for the determination of 2-D magnetic field, which is based on complex analysis theory [7]. Comparing with the conventional method usually used in approximation calculation, which is based on "assumed field pattern" mentioned in [1], [3]-[5], CM method has superior advantage in analytical computation. In the relative permeance functions (13), both of relative permeances for rotor saliency effect and slot opening effect considerations will be calculated by direct approach with the help of CM techniques [8].

The general aim of CM method is to choose an appropriate complex function for mapping transformation. If we assume that the original motor configurations placed in a complex plane **Z**, then by the conformal transformation function $z = f(w)$, the new simple configuration will be rebuilt in another complex plane **W**, where the field can be solved analytically. A sequence of several CM can be applied if necessary [7].

1) Saliency Effect

A CM is used to transform the cylindrical rotor to a square so that the effective air-gap length determined by flux path in PM can be calculated.

The rotor region placed in the original **Z**-plane is expressed by (14), in the form of logarithm equation, which

is composed of amplitude part and angle part. This expression satisfies the Cauchy-Riemann equation, i.e. [3],

$$f(z) = Log(z) = \ln|z| + jArg(z) \tag{14}$$

The function $Log(z)$ is not only continuous in the domain D, but also analytical in that domain, with the property:

$$\frac{d}{dz} Log(z) = \frac{1}{z} \neq 0 \tag{15}$$

where $D = \{z|: |z| > 0, \quad -\pi < Arg(\theta) < \pi\}$

Since, the image of any point (x, y) in the **Z**-plane is the point (u, v) in **W**-plane, whose rectangular coordinate is defined respectively by the following CM equation:

$$\begin{cases} u(x,y) = \frac{1}{2}\ln(x^2 + y^2) \\ v(x,y) = \arctan(y/x) \end{cases} \tag{16}$$

According to this CM function, 1/8 of the rotor region in the original **Z**-plan is conformal transformed into **W**-plane, Fig. 4 shows the transformed mapping region:

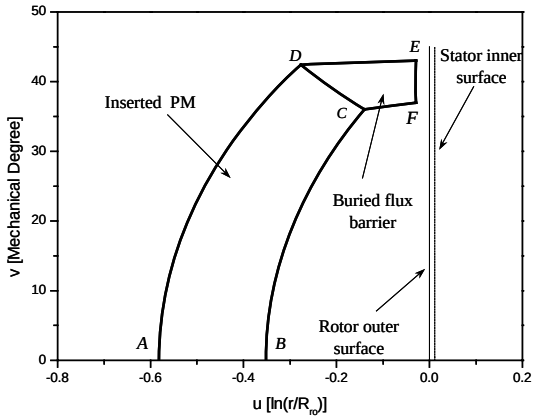

Fig. 4. Conformal Mapping of rotor cross-section of the IPM model

In the mapping region, for every interval on v-axis, the transformed air-gap length $G_{map}(\theta)$ for the flux lines in the direction of u-axis is calculated. Furthermore, the total air-gap length function, and the relative permeance $\lambda_{rotor-saliency}$ including the rotor saliency effect is given by means of Fig. 4 as follows [3]:

$$G(\theta) = g_0 + G_{map}(\theta) \tag{17}$$

$$\lambda_{rotor-saliency} = \frac{G_0}{G(\theta)} \tag{18}$$

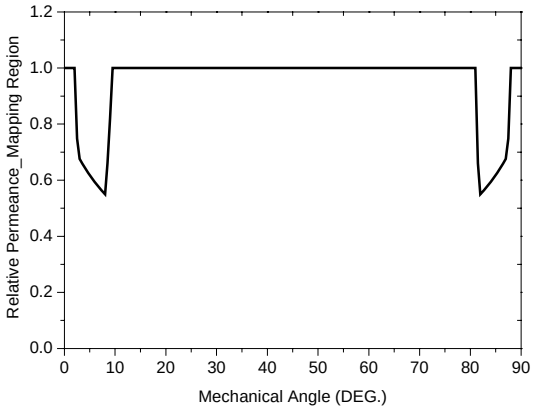

Fig. 5. Rotor saliency relative permeance distribution

In the above formula,

$$G_0 = g_0 + (h_m/\mu_r) \tag{19}$$

Depending on the magnetization direction of the PM, the flux passes through the inner of PM by different crossing paths: radial crossing and parallel crossing. Consequently the energy loss in the PM is different. In this paper, a parallel magnetization PM is chosen, so the flux lines in PM inner area are constant air-gap length, whose effective value is h_m/μ_r. The relative permeance distribution of parallel magnetization in this mapping approach is shown in Fig. 5.

2) Slot Opening Effect

Stator slots have a great effect on the flux density distribution in the air-gap, furthermore it affects the output performance. Therefore, either for air-gap field analysis, or for motor design, slot opening area should be precisely calculated.

A CM used for slots effect analysis is that transforms the complex upper half-plane (as Fig. 6(b) shows) to the interior of a polygon (such as the polygon in Fig. 6(a) created by the path 1-2-3-4-5), which means a simplified slot opening area obey the assumption (b). Since the air-gap is quit small compared with the width of slot opening, it is sufficient in the analysis to consider a singular slot area, and as far as the air-gap field is concerned, the slot opening area can be treated as infinitely deep, as Fig. 6(a) shows [7].

This CM transformation equation is obtained from Schwarz-Christoffel transform theory [7]-[9] giving as:

$$z = f(w) = \frac{2g_0}{\pi}\left[\frac{\beta}{2g_0}\arcsin\frac{w}{a} + \frac{1}{2}\log\frac{\sqrt{a^2 - w^2} + \frac{2g_0}{\beta}w}{\sqrt{a^2 - w^2} - \frac{2g_0}{\beta}w}\right] \tag{20}$$

where

$$a = \sqrt{1 + \left(\frac{2g_0}{\beta}\right)^2} \tag{21}$$

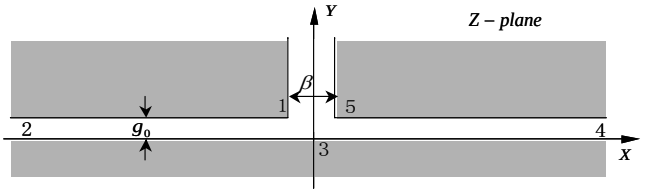

(a). Simplified singular slot opening configuration in Z-plane

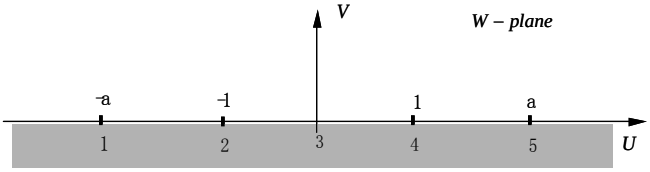

(b). Conformal mapping region of singular slot opening in W-plane

Fig. 6. Conformal mapping of IPM model stator slot opening

Now, the singular slot opening area in the **Z**-plane is mapped into the **W**-plane by the CM function (20). So, the magnetic field in slot opening area can be analyzed in the new plane. In the **W**-plane, an equivalent magnetic field is assumed setting along the real axis region [-1,1], which corresponding to the rotor surface in the **Z**-plane. It is in place of the magnetic flux source produced by the interior PM. The field can be expressed as [7]- [9]:

$$t = \frac{\varphi_{map}}{\pi} \ln\left(\frac{1+w}{1-w}\right) \tag{22}$$

Then, the flux density in the air-gap region is calculated from the given field, and the permeance $\lambda(x,y)$ can be obtained from the flux density by setting unit difference in the magnetic field between stator and rotor [9]. Hence:

$$B_{air-gap} = \mu_0 \frac{dt}{dz} = \mu_0 \frac{dt}{dw}\frac{dw}{dz} = \frac{2\mu_0 \cdot \varphi_{map}}{\beta_0 \sqrt{a^2 - w^2}} \tag{23}$$

$$\lambda_{stator-slots} = \frac{B_{air-gap}}{\varphi_{map}} = \frac{2\mu_0}{\beta_0 \sqrt{a^2 - w^2}} \tag{24}$$

Subsequently the relative permeance function $\lambda_{slot-effect}$ can be obtained by dividing $\lambda_{stator-slots}$ by a one-dimensional permeance function of an equivalent slotless stator IPM motor, as follows:

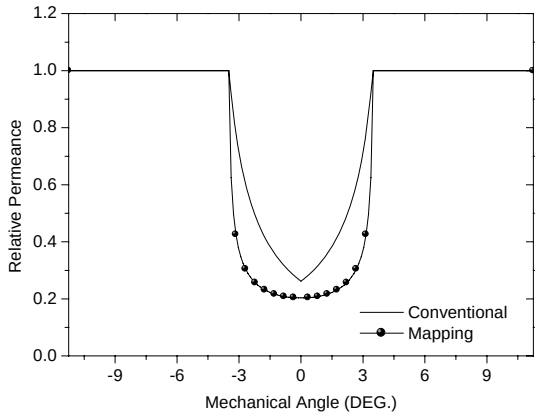

Fig. 7. A slot opening area relative permeance distribution

$$\lambda_{slot-effect} = \frac{\lambda_{stator-slot}}{(\mu_0/g_0)} = \frac{2g_0}{\beta_0 \sqrt{a^2 - w^2}} \tag{25}$$

The relative permeance results from the CM method and from "assumed field pattern" method used in [1], [4]-[5] are compared in Fig. 7. From the comparison, by these two approaches, the difference of slot opening effect on the flux density distribution along the stator wall surfaces is obviously observed. According to the Maxwell's tensor theory [7], cogging torque is determined by the flux density distribution along the stator surface [10]. Therefore, there is an error between these two methods. In this paper, the relative permeance function getting from CM method is used in the presented analytical method. The accuracy of the CM method result will be proved in the flux density distribution comparison.

III. Result Comparison

To verify the accuracy of this developed analytical method, 2-D FEA is performed, and the results that from analytical calculation and FEA are compared. Fig. 8 shows the equi-potential (flux lines) distribution at a rotor position. Fig. 9 shows the comparison of the flux density distribution in the air-gap, which is correspond with the parallel magnetization of IPM. With a good agreement in flux density comparison, cogging torque of the IPM model is calculated, based on flux density distribution, and it is compared with FEA, as shown in Fig. 10. From the comparisons, this developed analytical method is well proved.

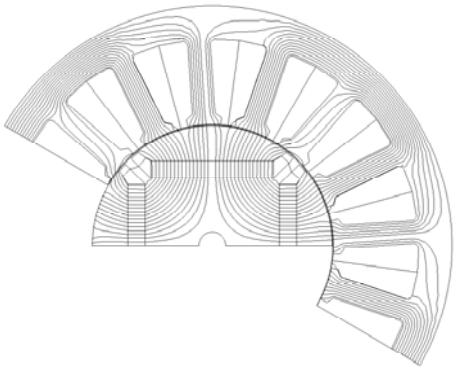

Fig. 8 Equi-potential distribution in FEA model

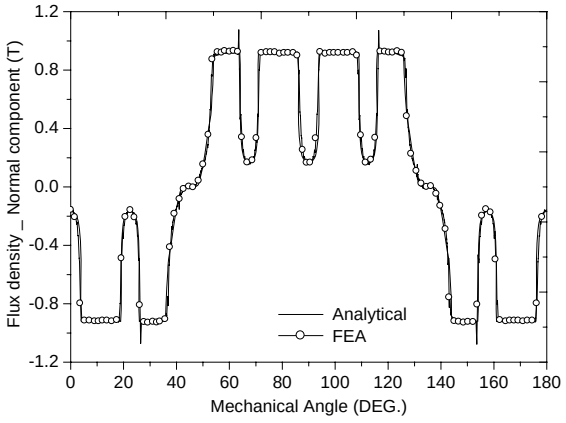

Fig. 9 Comparison of flux density distribution in air-gap field

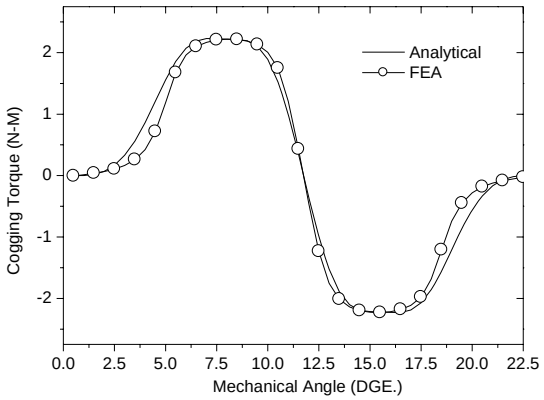

Fig. 10. Comparison of calculated and FEA cogging torque

IV. Conclusion

An analytical method used to predict the air-gap field distribution in an IPM motor is improved by using conformal mapping techniques in this paper. With the help of the conformal mapping techniques, stator slots effect and rotor saliency effect on the field distribution are well considered. The good agreement of results comparison from both analytical method and FEA simulation verifies the accuracy of the analytical method. The proved analytical method can give well support to motor characteristic analysis, and initial motor design of IPM motors.

Appendix
List of Symbols And Motor Parameters

R_s	Inner radius of stator	45.5(mm)
R_r	Radius of rotor	45 (mm)
R_m	Effective radius of magnet	38.5(mm)
h_m	Height of PM	6.5 (mm)
g_0	Length of air-gap	2 (mm)
β_0	Slot opening width	5.8 (mm)
L	Length of stack	87 (mm)
n_s	Number of slots	16
α_f	Flux barrier angle	76 (deg.)
α_p	Pole-arc angle	72 (deg.)
y	Magnetic rib width	0.5 (mm)
B_r	PM remanent induction	1.1 (T)
B_s	Saturation flux density	2.0 (T)
μ_0	Vacuum relative permeability	1
μ_r	PM relative permeability	1.05

Acknowledgment

This work was supported by grant No. RTI04-01-03 from the Regional Technology Innovation Program of the Ministry of Commerce, Industry and Energy(MOCIE).

References

[1] Gyu-Hong Kang, Jung-Pyo Hong and Gyu-Tak Kim, "Analysis of Cogging Torque in Interior Permanent Magnet Motor by Analytical Method," J*ournal of KIEE.* 11B. 1-8 (2001)

[2] Nicola Bianchi and Thomas M. Jahns, *Design, Analysis, and Control of Interior PM Synchronous Machines.* IEEE Industry Applications Society Annual Metting Seattle, USA, October 3rd, 2004

[3] A. Kiyoumarsi and M. Moallem, "A New Analytical method on the Field Calculation of Interior Permanent-Magnet Synchronous Motor," Isfahan University of Technology, isfahan, Iran, 84154.

[4] Z.Q. Zhu, "Instantaneous magnetic field distribution in brushless permanent magnet dc motors. Part 3, Effect of stator slotting," *IEEE Trans. Magn.*, vol.29, pp143-151, Jan 1993

[5] Z.Q. Zhu, D. Howe, "Analytical prediction of the cogging torque in radial-field permanent magnet brushless motors," *IEEE Trans. Magn.*, vol.28, no.2. pp1317-1374.

[6] Boldea I. and Nasar S.. The Induction Machine Handbook, chapters 12-14, CRC Press, 2002.

[7] Miroslav Markovic, Marcel Jufer and Yves Perriard "Reducing the Cogging Torque in Brushless DC Motors by Using Conformal Mappings," *IEEE Transactions on Magnetics.*, vol.40, no.2, March.2002.

[8] K. J. NINNS and P. J. LAWRENSON. *Analysis and Computation of Electric and Magnetic Field Problems* (SECOND EDNITION), chapter 8, PERGAMON PRESS, 1973.

[9] S. L. HO and Y. J. ZHANG and G. D. XIE "Two-dimensional analytical method to predict the electromagnetic field of Disc-type permanent magnet machines," *Electric Machines and Power Systems*, 26:649-658, 1998.